Accurate Band Alignment of Sputtered Sc_2O_3 on GaN for High Electron Mobility Transistor Applications

Partha Das[1,*], Harry Finch[2], Holly J. Edwards[3], Saeed Almalki[2], Vinod R. Dhanak[4], Rajat Mahapatra[5] and Ivona Z. Mitrovic[2,*]

[1] Department of Electronics Engineering, Sardar Vallabhbhai National Institute of Technology, Surat, 395007, India
[2]Department of Electrical Engineering & Electronics, University of Liverpool, Liverpool L69 3GJ, United Kingdom
[3]The Lab at Brookes Bell, Birkenhead CH41 7ED, United Kingdom
[4]Department of Physics and Stephenson Institute for Renewable Energy, University of Liverpool, Liverpool L69 7ZF, United Kingdom
[5]Department of Electronics and Communication Engineering, National Institute of Technology, Durgapur, 713209, India

*E-mail: pd@eced.svnit.ac.in, ivona@liverpool.ac.uk

Received xxxxxx
Accepted for publication xxxxxx
Published xxxxxx

Abstract

Sc_2O_3 is a promising gate dielectric for surface passivation in GaN-based devices. However, the interface quality and band alignment of sputtered Sc_2O_3 on GaN is not fully explored. In this work, X-ray photoelectron spectroscopy (XPS) and variable angle spectroscopic ellipsometry (VASE) were performed to extract the discontinuities in the valence and conduction band of Sc_2O_3/GaN system. Sc_2O_3 films were deposited on GaN using radio frequency sputtering. The valence band offset of Sc_2O_3/GaN was deterimened to be 0.76 ± 0.1 eV using Kraut's method. The Sc_2O_3 band gap of 6.03 ± 0.25 eV has been measured using O 1s energy loss spectroscopy. The electron affinity measurements of GaN and Sc_2O_3 using XPS secondary electron cut-off spectra provide additional degree of accuracy to derived band line-up for Sc_2O_3/GaN interface. The band alignment results are compared with literature values of band offsets determined experimentally and theoretically for differently grown Sc_2O_3 films on GaN.

Keywords: band offsets, GaN, high-κ oxides, Kraut's method, variable angle spectroscopic ellipsometry, X-ray photoelectron spectroscopy

1. Introduction

Gallium nitride (GaN) is a wide band gap (WBG) material that is a focal point of contemporary research for its application in high electron mobility transistor (HEMT) due to the formation of 2-dimensional electron gas (2DEG) at AlGaN/GaN heterojunction [1–3]. Such devices have lower on-state resistances and with added material benefits of GaN are expected to outperform Si based counterparts for high voltage and high-power switching applications. Moreover, it has a reasonably high thermal conductivity, compared to that of Si, which is important for high-temperature power device applications [4]. The conventional gallium nitride based

HEMT devices are inherently depletion mode (d-mode), i.e. device is normally on at zero gate to source voltage (V_{GS}). In order to compete with the commercially accessible Si technology, GaN devices must be enhancement-mode (e-mode) or normally-off. Low off-currents are required for e-mode devices to minimise static power consumption, provide fail-safe operation and have a significant gate voltage swing [5]. Typically, these devices take the form of metal-insulator-semiconductor (MIS)-HEMT or MIS-field-effect-transistor (FET), where the insulating dielectric is placed between gate metal and the AlGaN barrier layer or GaN cap layer. The incorporation of various dielectrics such as SiO_2 [6,7], Al_2O_3 [8,9], HfO_2 [10], ZrO_2 [11,12], Ta_2O_5 [13,14], TiO_2 [15,16], Ga_2O_3 [17] and $LaLuO_3$ [18], AlON [19], Si_3N_4 [20] amongst others have been investigated for inclusion in MIS-HEMTs.

The MIS-HEMT has been comprehensively investigated as a promising power switching device after being initially studied for radio frequency (RF) applications [21]. Due to MIS-gate, transistors are more resilient to gate voltage over-shoot and hence suitable for high frequency power switching. However, introduction of gate dielectric materials to the GaN-based heterostructures can degrade the device performance in a number of ways. Interface trap charges can affect device performance by serving as distant impurity scattering centers, which can either affect the threshold voltage [22] or lower the mobility of the carriers [23]. Switching performance is also affected by threshold voltage instability, large hysteresis and current collapse caused by the fast charging and discharging of the trap states [24,25]. Additionally, the oxide/GaN heterostructure system should have large valence band and conduction band offsets to improve the semiconductor carrier confinement's characteristics [26]. Large band gap high-κ dielectrics can provide larger tunneling barriers for carriers, therefore reducing gate leakage. To increase the electrostatic control over the channel and the on-current, which in turn leads to higher transconductance, high-κ material is required. Therefore, it is essential to choose dielectric material correctly using the above given criteria.

There are limited reports of amorphous Sc_2O_3 processed either by atomic layer deposition (ALD) or sputtering for use in MIS-HEMTs. A low process temperature is required for deposition of high-κ dielectrics for use in MIS-HEMTs [27]. It has been reported that the as-deposited ALD processed amorphous Al_2O_3 changes to polycrystalline after annealing at 800°C, causing large increase in the leakage current of the Al_2O_3/GaN structure [28]. Hence, the low processing temperature of high-κ dielectric is a paramount, to ensure its amorphous nature.

This paper focuses on photoelectron emission study of room temperature fabricated Sc_2O_3 films, inherently amorphous. The band alignment of only crystalline Sc_2O_3 on GaN has been reported in the literature [29-31]. Chen *et al.* reported Sc_2O_3 deposited by RF plasma-enhanced molecular beam epitaxy (MBE) having a bixbyite crystalline structure [29]. It has been stated that when grown at a substrate temperature of 100°C, the single crystalline nature of Sc_2O_3 film is lost after a few nanometers leaving the remaining growth as polycrystalline [29]. The Mg X-source with energy of 1253.6 eV was used in the X-ray photoelectron spectroscopy (XPS) measurements on three samples: 3 μm GaN on sapphire, 40 nm Sc_2O_3/GaN and 3 nm Sc_2O_3/GaN [29]. There is no evidence of how band gap of Sc_2O_3 film was measured in [29], but the value of 6.0 eV was used to state the conduction band offset (CBO). The binding energies (BEs) of shallow core levels (CLs) of Ga 3d and Sc 3p were used to determine 0.42 ± 0.07 eV valence band discontinuity (ΔE_V) or valence band offset (VBO) at Sc_2O_3/GaN interface using Kraut's equation [32]

$$\Delta E_V = VBO = \Delta_{substrate} + \Delta_{interface} - \Delta_{oxide} \quad (1)$$

where, $\Delta_{substrate}=\Delta_{GaN}$ = Ga 3d – VBM_{GaN}= 17.62 eV, Δ_{oxide} = Sc 3p – VBM_{Sc2O3}= 28.65 eV and $\Delta_{interface}$=Sc 3p – Ga 3d = 11.45 eV. Note that VBM refers to valence band maximum and refers to the position of Fermi level in a substrate (here GaN) or bulk oxide (here Sc_2O_3). Liu *et al*. [31] have presented XPS study of pulsed-laser-deposition (PLD) grown Sc_2O_3/GaN heterostructure using same shallow CLs as in [29]. The X-ray diffraction study confirmed crystalline nature of deposited Sc_2O_3 films with low leakage current of 1 μA/cm^2 at a reverse gate bias of 30 V in 100 nm Sc_2O_3/GaN MIS devices [30]. Liu *et al.* [31] have used a monochromatic Al K-α source at 1486.6 eV for XPS measurements on GaN/sapphire, 100 nm Sc_2O_3/GaN and 3 nm Sc_2O_3/GaN samples and reported the VBO of 0.84 ± 0.05 eV using the following measured values of Δ_{GaN} = Ga 3d – VBM_{GaN}= 17.54 eV, Δ_{oxide} = Sc 3p – VBM_{Sc2O3}= 28.37 eV and $\Delta_{interface}$ = Sc 3p -Ga 3d = 11.67 eV. Moreover, the XPS experimental study in [31] was validated using simulated and experimental valence band (VB) spectra for Sc_2O_3/GaN heterostructure, showing good agreement. The full band line-up of crystalline Sc_2O_3/GaN in [31] was derived by taking values of band gap of Sc_2O_3 of 6.3 eV from the literature [33], not measured. Afanas'ev *et al.* [34] have measured optical band gap by visible-ultra violet (UV) spectroscopic ellipsometry (SE) of both, crystalline and amorphous Sc_2O_3 films, and found values of 6.0-6.1 eV and 5.6-5.7 eV, respectively. Similar value of 6.0 eV has been reported for single crystals of nominally pure Sc_2O_3 using UV absorption spectra [35]. In more recent study, Dixon *et al.* [36] have reported band gaps of amorphous and crystalline Sc_2O_3 of 5.3 eV and 5.7 eV, respectively using diffuse reflectance measurements. It is likely that the lower values of band gap reported in [36] is due to using aerosol-assisted chemical vapour deposition (CVD) at 550°C, where varying degrees of crystallinity of the deposited Sc_2O_3 films due to varying of the oxidising character of the deposition environment reduces the band gap significantly.

Further to the state of the art detailed above, this paper presents comprehensive band alignment study of Sc_2O_3/GaN heterointerface with novel contributions in the following three aspects: (i) the Sc_2O_3 films were prepared using room temperature RF sputtering and hence inherently amorphous to facilitate low leakage current in MIS-HEMT devices; (ii) the photoemission experiments and associated analysis were done using deep core levels of Ga 2p and Sc 2p, that have not been previously reported; (iii) the additional XPS measurements were performed to find secondary electron cut-off (SEC) and hence determine ionisation energy of both GaN and Sc_2O_3. Since the band gap of GaN and sputtered Sc_2O_3 were measured using variable angle spectroscopic ellipsometry (VASE) and XPS O 1s energy loss spectroscopy, respectively, the electron affinity was determined experimentally for GaN and sputtered Sc_2O_3, substantiating the band alignment findings using Kraut's method. The latter renders experimental findings in this study more comprehensive than what has been reported in the literature [29-31] using only Kraut's method.

The results point to suitable valence and conduction band offsets at Sc_2O_3/GaN of 0.76 eV and 1.89 eV, respectively to prevent electron and hole tunneling in associated MIS-HEMT devices.

2. Experimental

The 5 μm un-doped GaN (0001) on c-plane sapphire (purchased commercially) was used as a substrate sample. As received, its surface would have been contaminated with oxygen and carbon, therefore it was cleaned with hydrochloric acid (HCl) followed by ultra-sonification for 10 minutes each in acetone followed by methanol, and finally rinsing with deionised (DI) water. To prepare the Sc_2O_3/GaN samples, Sc_2O_3 films (99.99% purity-purchased commercially) were RF magnetron sputter-coated at room temperature on a clean GaN/sapphire sample in a Moorfield nano-PVD (physical vapour deposition) apparatus using the deposition parameters listed in table 1.

Table 1: A summary of sputtering parameters used for deposition of Sc_2O_3/GaN samples.

Sputtering parameter	Value
Argon flow rate [sccm]	0.5
Sputtering power [W]	60
Chamber pressure [mbar]	1×10^{-3}
Sample-to-target distance [cm]	11
Deposition rate [$Å s^{-1}$]	0.04
Target diameter [mm]	50.8
Target thickness [mm]	3.18

Two samples were fabricated, with thin (3 nm nominal) Sc_2O_3 film and with thick (10 nm nominal) Sc_2O_3 film on GaN/sapphire substrate. The thick 10 nm film can be considered bulk-like as the inelastic mean free path of the photoelectrons at the kinetic energies used in the experiment is about 2.5 nm [37], and so all detected photoelectrons will have originated from the Sc_2O_3 layer. Reference samples of the same (thin and thick) Sc_2O_3 films on n-Si(100) were deposited simultaneously in the sputtering chamber to determine the oxide thickness and optical properties by variable angle spectroscopic ellipsometry. The VASE measurements were done at room temperature using a J. A. Woollam M2000 ellipsometer within the photon energy range of 0.7–5.1 eV (240-1700 nm) and three incidence angles (65°, 70° and 75°). The VASE experimental data comprise of Ψ (psi) vs. photon energy and delta (Δ) vs. photon energy that need to be fitted using spectroscopic ellipsometry model. The fitting was done using Complete Ease6.7 software programme [38].

XPS measurements were performed in an ultra high vacuum (UHV) chamber consisting of a SPECS Al-Kα (1486.6 eV) monochromator source, PSP hemispherical electron energy analyser and an Ar ion sputter source. The analyser was calibrated using the Ag 3d core levels and Fermi edge measured from a sputter cleaned Ag foil. The spectrometer was operated with an overall resolution of ± 0.1 eV. The spectra were charge corrected to the C 1s core level at 284.6 eV, and the line shapes fitted using Voigt functions after Shirley background subtraction, details of which can be found in [39,40].

3. VASE measurement results

Figures 1(a)-(b) show experimental and fitted (Ψ, Δ) vs. photon energy data for bulk Sc_2O_3/Si sample. The Sc_2O_3 film on Si is fitted using a Cauchy model defined as

$$n(\lambda) = A + \frac{B}{\lambda^2} + \frac{C}{\lambda^4}, \qquad (2)$$

where n is the refractive index, λ is wavelength, and A, B and C are Cauchy parameters. The film thickness is found to be 10.7 ± 0.1 nm close to the nominal value. The Cauchy model is then parametrised using B-spline to achieve good quality fitting. Applying the same fitting model, the thickness of the thin Sc_2O_3 sample is found to be 3.0 ± 0.1 nm. The quality of the fit is ascertained by mean squared error (MSE), being less than 5. The optical constants of Sc_2O_3 film, refractive index (n) and extension coefficient (k) as a function of photon energy, extracted from modelling data shown in figures 1(a)-(b), are shown in figure 1(c). No absorption was observed for Sc_2O_3 in the region of SE measurements, from 0.7 to 5.1 eV, that is k = 0, indicating that the band gap cannot be determined using VASE as it is higher than 5.1 eV. The refractive index is found to be ~1.9 eV for Sc_2O_3. Dixon *et al.* [36] have found n varying from 1.87 – 1.94 in the range 1.2 - 3.1 eV, with n = 1.89 at 550 nm (2.48 eV) for 350 nm amorphous Sc_2O_3, while

n for crystalline Sc_2O_3 has been found to be 2.00 [41]. For Sc_2O_3 films in this work, n at 550 nm is 1.9, indicating that the films are amorphous as expected.

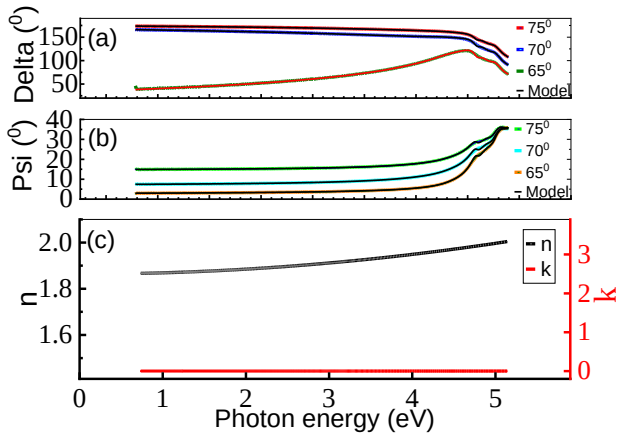

Figure 1. Spectroscopic ellipsometry data taken at 60˚-70˚ of (a) delta and (b) psi versus photon energy fitted using Cauchy model for the bulk Sc_2O_3 film on Si. (c) The refractive index, n and extinction coefficient, k for Sc_2O_3 film derived from fitted SE data shown in (a)-(b).

In case of VASE data for GaN/sapphire substrate, the fitting was done using Cody-Lorentz oscillator to model the GaN, and a transparent Cauchy layer for the surface overlayer due to exposure to air and subsequent growth of native oxide. The Cody-Lorentz model is chosen as it has an exponential absorption below the band gap energy, providing a more accurate model for GaN [42]. The thickness of GaN was found to be 4.62 μm and correlates to nominal 5 μm expected from the commercially produced wafer. An optimised fit with MSE of 12.2 was found when a surface roughness of 1.3 nm was introduced to the model, in agreement with the roughness determined by atomic force microscopy (AFM) (not shown). The Δ vs. photon energy experimental curve shown in figure 2(a) shows high frequency large amplitude oscillations below the band gap of 3.4 eV as a result of interference effects due to reflections at the GaN and sapphire boundaries [43]. These interference effects reduce in amplitude around the band gap value where there is a sharp increase in extinction coefficient value (see figure 2(b)) that monotonically increases with energy thereafter in the absorbing region. The band gap of GaN can then be extracted using Tauc relationship [44]

$$(\alpha h\nu)^{1/r} \propto (h\nu - E_g). \qquad (3)$$

α is absorption coefficient and can be found from extinction coefficient as

$$\alpha = \frac{4\pi k(E)E}{hc}, \qquad (4)$$

where E = hν is photon energy, h is Planck's constant, and c is speed of light. The coefficient r is 1/2 due to direct allowed transition that GaN is known to have [45].

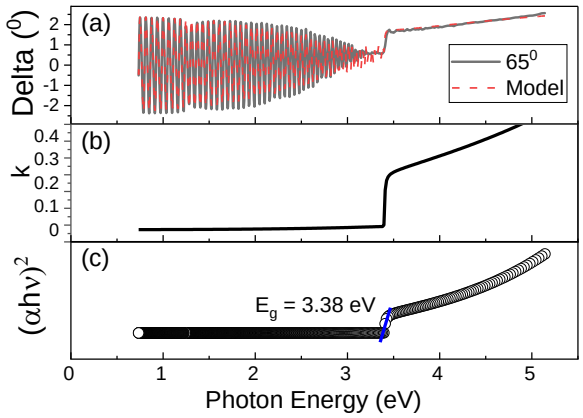

Figure 2. (a) SE data of Δ vs. photon energy taken at 65˚ and fitted using Cody-Lorentz oscillator model for 4.6 μm GaN/sapphire sample. (b) Extinction coefficient, k vs. photon energy and (c) Tauc plot for GaN derived from fitting shown in (a). The Tauc plot depicts extraction of GaN band gap.

Hence, the band gap (E_g) of GaN is extracted from the Tauc plot shown in figure 2(c) using linear extrapolation of the leading edge to the baseline and found to be 3.38 ± 0.1 eV. The latter agrees closely to values published in the literature for wurtzite GaN of 3.4 eV to 3.44 eV [43,46-48].

4. XPS measurement results and discussion

4.1 XPS measurements of cleaned GaN substrate

Prior to measuring XPS from bulk GaN, after the ex-situ chemical cleaning detailed previously, the substrate sample was sputtered in-situ using Ar^+ ions at 500 eV for about 5 minutes, in a grazing incidence geometry in order to remove any surface oxides and carbon related impurities. The Ga $2p_{3/2}$ core level and valence band spectra of GaN substrate are shown in figure 3. Ga $2p_{3/2}$ CL has been fitted by three components attributed to Ga-N, Ga-O and Ga-Ga bonds.

The bulk Ga $2p_{3/2}$ line shape consists of a small peak on the right at 1117 eV attributed to Ga-Ga bonds from non-stoichiometric GaN at the surface. There is also a small peak at 1119.1 eV attributed to surface Ga_2O_3. Due to the strong oxygen affinity of a clean GaN surface, the small Ga_2O_3 peak confirms the presence of a native oxide, indicating its reoxidation during the brief ambient exposure between wet chemical cleaning and XPS measurement [49,50]. The peak position of the Ga $2p_{3/2}$ CL corresponding to Ga-N bond was found to be at 1118.30 eV.

The Ga 2p CL was chosen for XPS analysis using Kraut's method of the bulk GaN substrate rather than Ga 3d due to the reason that the Ga 3d semi-core level has low binding energy and has a propensity to hybridize with s-levels at the VB edge. The VBM was determined to be 3.08 eV from the intersection

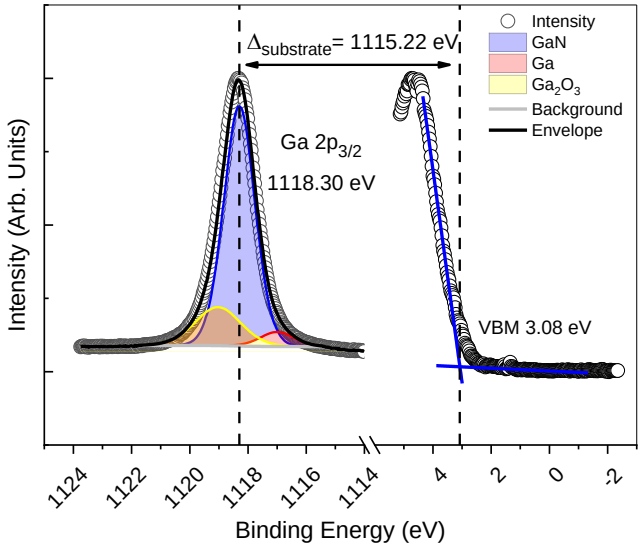

Figure 3. XPS Ga 2p CL and VB spectra of GaN substrate.

of linear fitting of the rising edge and the background. For cleaned GaN substrate, the difference between the BEs of Ga 2p CL and VBM ($\Delta_{substrate}$) is found to be 1115.22 eV.

4.2 XPS measurements of bulk Sc_2O_3 sample

Sc $2p_{3/2}$ CL and the VB spectra for the bulk Sc_2O_3/GaN sample are shown in figure 4. The peak position of Sc $2p_{3/2}$ CL (for Kraut's method) was found to be 401.01 eV and the corresponding VBM was determined to be 2.06 eV. The difference in BEs between the Sc $2p_{3/2}$ CL and VBM for thick Sc_2O_3 sample (Δ_{oxide}) was extracted to be 398.95 eV.

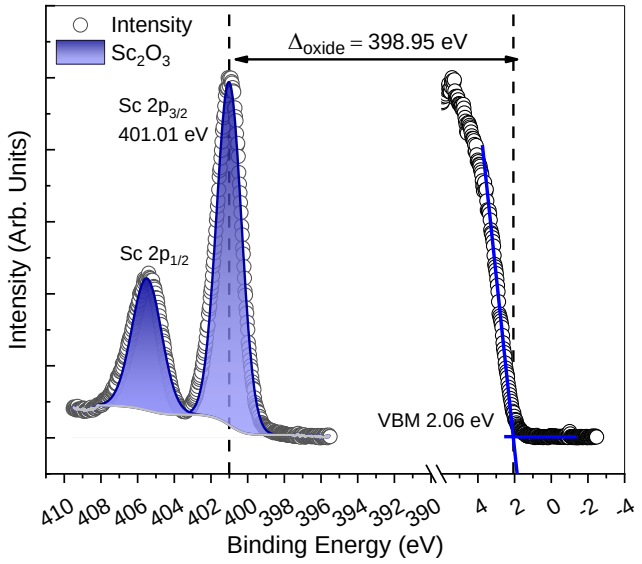

Figure 4. Sc $2p_{3/2}$ CL and VB spectra of bulk Sc_2O_3 sample.

Sc_2O_3 film band gap was determined by measuring the onset of XPS O 1s energy loss spectrum of bulk sample as explained by Nichols *et al.* [51]. The band gap of Sc_2O_3 was extracted to be 6.03 ± 0.25 eV as shown in figure 5(a). The error bar of ± 0.25 eV is due to uncertainty in linear interpolation of rising edge of electron energy loss on high binding energy side of O 1s CL.

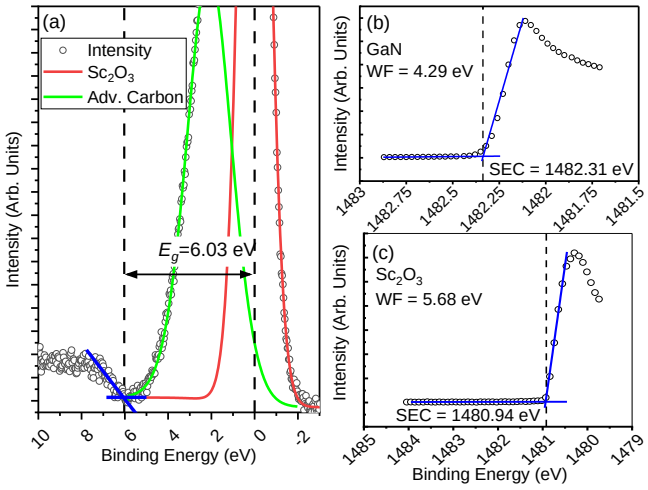

Figure 5. (a) Band gap of sputtered Sc_2O_3 layer derived from O 1s loss spectroscopy; Secondary electron cut-off spectra for (b) GaN substrate and (c) bulk Sc_2O_3 film.

Figures 5(b)-(c) show the secondary electron cut-off spectra of GaN and bulk Sc_2O_3 samples. The SEC measurements were done by first biasing the sample to differentiate the SEC values of the sample and the analyser, with the nominal value of applied bias, V_{app} ~ -10 V, and then measuring the SEC edge and a reference core level under the same conditions. Once adjusted for the energy shift, the SEC value can be determined by linear intersection of the edge with the spectrum background as shown in figures 5(b)-(c). The work function, WF=qϕ defined as difference between the Fermi and vacuum levels, can be determined as

$$q\phi = 1486.6\ \text{eV} - (SEC + qV_{app}), \qquad (5)$$

where 1486.6 eV refers to the X-ray energy of Al K-α source. Note that in figures 5(b)-(c) the x-axes of BEs were adjusted for applied bias, V_{app}. The electron affinity, χ can then be determined as

$$\chi = IE - E_g = (q\phi + VBM) - E_g \qquad (6)$$

where VBM refers to value extracted either from figure 3 or figure 4. The electron affinity (± 0.25 eV) is found to 3.99 eV for GaN and 1.71 eV for Sc_2O_3, using equation (6) and measured values of work function (figures 5(b)-(c)), VBM (figures 3 and 4) and band gap (figures 2(c) and 5(a)). The electron affinity of sputtered Sc_2O_3 of 1.71 ± 0.25 eV reported here is lower than theoretically predicted range of 1.98-2.5 eV [52], and also lower than 2.06 eV value [53], deduced from

internal photoemission and UV-SE measurements on Sc_2O_3/Si sample [34].

4.3 XPS measurements of interfacial Sc_2O_3/GaN sample

Figure 6 shows the Ga 2p and Sc 2p CL spectra for thin Sc_2O_3 on GaN sample measured by XPS. This fitting resulted in binding energies attributed to Ga-N (1116.90 eV) and Sc-O (401.39 eV) for interfacial sample. The CL difference, $\Delta_{interface}$ for the interfacial Sc_2O_3/GaN sample was determined to be 715.51 eV. It is noted that the N 1s line shape from GaN is complicated by the presence of Ga Auger peaks.

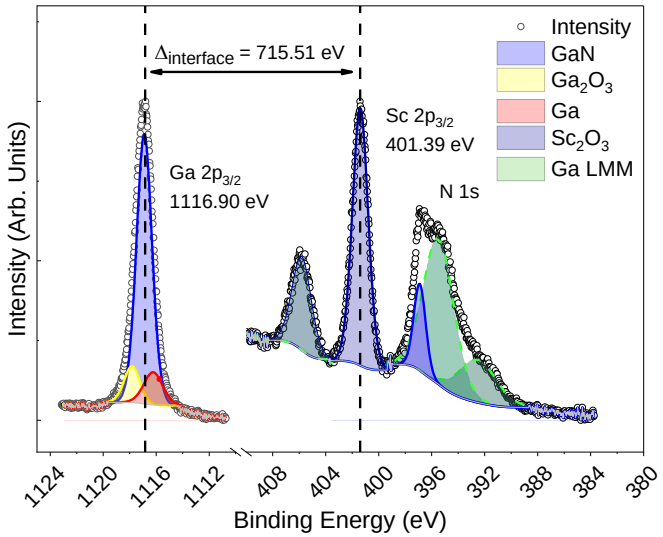

Figure 6. Fitted Ga 2p and Sc 2p CL spectra showing calculation of $\Delta_{interface}$ for interfacial Sc_2O_3/GaN sample.

4.4 Band alignment of Sc_2O_3 on GaN

The valence band discontinuity ΔE_V for sputtered Sc_2O_3 can be determined using equation (1) by inserting values of $\Delta_{substrate}$ (figure 3), Δ_{oxide} (figure 4) and $\Delta_{interface}$ (figure 6). The conduction band discontinuity, ΔE_C or CBO can then be calculated using

$$\Delta E_C = CBO = E_g^{oxide} - E_g^{GaN} - \Delta E_V \qquad (7)$$

where E_g^{oxide} and E_g^{GaN} are the band gap values of Sc_2O_3 and GaN substrate, respectively. The valance band offset of sputtered Sc_2O_3 on GaN is found to be 0.76 ± 0.1 eV, while the corresponding conduction band offset is determined to be 1.89 ± 0.1 eV using equation (7). Taking into account the measured χ for GaN and Sc_2O_3, the CBO value is slightly higher (2.28 eV) than what is extracted using Kraut's method (1.89 eV, equation (1)). This discrepancy cannot be explained by measurement error (typically ± 0.25 eV when extracting the band gap from O 1s energy loss spectrum, which also affects the calculated value of χ). It is likely that some upward band bending (BB) could be present at Sc_2O_3/GaN heterointerface, however further angle resolved (AR)-XPS measurements are required to corroborate this. The VBO of 0.76 ± 0.1 eV for sputtered Sc_2O_3/GaN in this study closely correlates to 0.84 ± 0.05 eV measured for crystalline pulsed laser deposited Sc_2O_3/GaN [31]. The XPS experimentally obtained VBO values in this study and in [31] agree with most recent theoretically predicted values obtained using density functional supercell calculation (0.81 eV, [54]) and using dielectric dependent hybrid functional theory (0.93 eV [55]) as summarised in figure 7.

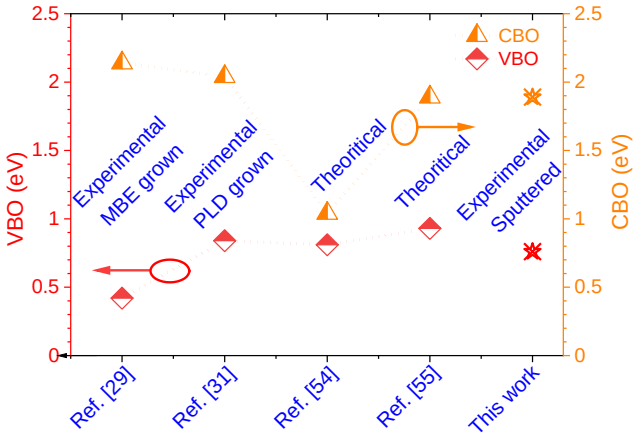

Figure 7. Comparison of VBO and CBO obtained for Sc_2O_3/GaN interface in this study and literature [29,31,54,55].

The complete band alignment of sputtered Sc_2O_3/GaN is shown in figure 8.

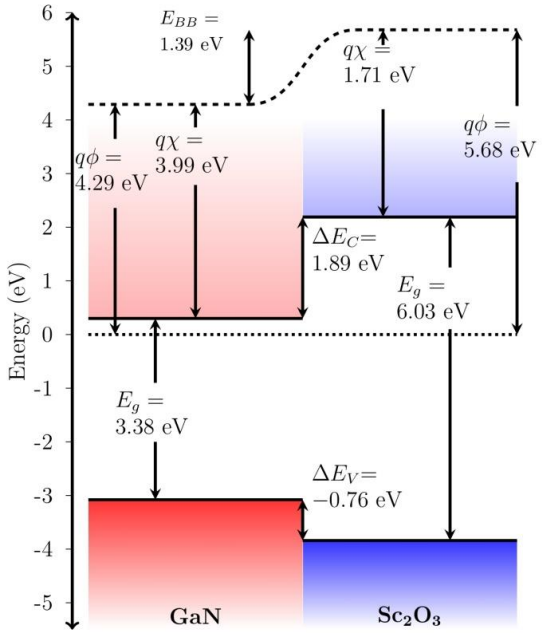

Figure 8. Schematic of band line-up of sputtered Sc_2O_3/GaN where the Fermi levels in both GaN and Sc_2O_3 are aligned.

5. Conclusion

The valence band offset of sputtered Sc_2O_3/GaN heterojunction has been determined to be 0.76 ± 0.1 eV with corresponding conduction band offset of 1.89 ± 0.1 eV forming a type I "straddling interface". The significance of the results in this paper refer to high-temperature operation regime, where GaN-based MIS devices with amorphous low temperature deposited sputtered Sc_2O_3 insulator film, as gate dielectric, may effectively confine electrons thanks to the appreciable conduction band offset.

Acknowledgements

This work is supported in part by the GCRF 'Digital in India' project no. EP/P510981/1 and UKRI GIAA award funded by the EPSRC, UK and UGC-UKIERI project no. F.No.184-1/2018 (IC) and IND/CONT/G/17-18/18 funded by the British Council. IZM acknowledges EPSRC Impact Acceleration Award 2023-2024, grant no. EP/X525741/1, UK.

References

[1] Amano H, Baines Y, Beam E, Borga M, Bouchet T, Chalker P R, Charles M, Chen K J, Chowdhury N, Chu R, De Santi C, De Souza M M, Decoutere S, Di Cioccio L, Eckardt B, Egawa T, Fay P, Freedsman J J, Guido L, Häberlen O, Haynes G, Heckel T, Hemakumara D, Houston P, Hu J, Hua M, Huang Q, Huang A, Jiang S, Kawai H, Kinzer D, Kuball M, Kumar A, Lee K B, Li X, Marcon D, März M, McCarthy R, Meneghesso G, Meneghini M, Morvan E, Nakajima A, Narayanan E M S, Oliver S, Palacios T, Piedra D, Plissonnier M, Reddy R, Sun M, Thayne I, Torres A, Trivellin N, Unni V, Uren M J, Van Hove M, Wallis D J, Wang J, Xie J, Yagi S, Yang S, Youtsey C, Yu R, Zanoni E, Zeltner S and Zhang Y 2018 The 2018 GaN power electronics roadmap *J. Phys. D. Appl. Phys.* **51** 163001

[2] Chen K J and Zhou C 2011 Enhancement-mode AlGaN/GaN HEMT and MIS-HEMT technology *Phys. Status Solidi Appl. Mater. Sci.* **208** 434–8

[3] Disney D, Letavic T and Trajkovic T 2017 High-voltage integrated circuits : history , state of the art, and future prospects *IEEE Trans. Electron Devices* **64** 659–73

[4] Paskov P P, Slomski M, Leach J H, Muth J F and Paskova T 2017 Effect of Si doping on the thermal conductivity of bulk GaN at elevated temperatures – theory and experiment *AIP Advances* **7** 095302 -1-15

[5] Chen K J, Yang S, Liu S, Liu C and Hua M 2016 Toward reliable MIS- and MOS-gate structures for GaN lateral power devices *Phys. Status Solidi A* **213** 861–7

[6] Kordoš P, Heidelberger G, Bernát J, Fox A, Marso M and Lüth H 2005 High-power SiO_2/AlGaN/GaN metal-oxide-semiconductor heterostructure field-effect transistors *Appl. Phys. Lett.* **87** 143501

[7] Arulkumaran S, Egawa T, Ishikawa H, Jimbo T, Sano Y, Arulkumaran S, Egawa T, Ishikawa H and Jimbo T 2004 Surface passivation effects on AlGaN/GaN high-electron-mobility transistors with SiO_2, Si_3N_4, and silicon oxynitride *Appl. Phys. Lett.* **84** 613

[8] Ye P D, Yang B, Ng K K, Bude J, Wilk G D, Halder S and Hwang J C M 2005 GaN metal-oxide-semiconductor high-electron-mobility-transistor with atomic layer deposited Al_2O_3 as gate dielectric *Appl. Phys. Lett.* **86** 063501

[9] Hashizume T, Anantathanasarn S, Negoro N, Sano E, Hasegawa H, Kumakura K and Makimoto T 2004 Al_2O_3 insulated-gate structure for AlGaN/GaN heterostructure field effect transistors having thin AlGaN barrier layer *Jpn. J. Appl. Phys.* **43** L777–9

[10] Tian F and Chor E F 2010 Improved electrical performance and thermal stability of HfO_2/Al_2O_3 bilayer over HfO_2 gate dielectric AlGaN/GaN MIS–HFETs *J. Electrochem. Soc.* **157** H557–61

[11] Jiang H, Liu C, Ng K W, Tang C W and Lao K M 2018 High-performance AlGaN/GaN/Si Power MOSHEMTs with ZrO_2 gate dielectric *IEEE Trans. Electron Devices* **65** 5337–42

[12] Anderson T J, Wheeler V D, Shahin D I, Tadjer M J, Koehler A D, Hobart K D, Christou A, Kub F J and Eddy C R 2016 Enhancement mode AlGaN/GaN MOS high-electron-mobility transistors with ZrO_2 gate dielectric deposited by atomic layer deposition *Appl. Phys. Express* **9** 071003

[13] Deen D A, Storm D F, Bass R, Meyer D J, Katzer D S, Binari S C, Lacis J W and Gougousi T 2011 Atomic layer deposited Ta_2O_5 gate insulation for enhancing breakdown voltage of AlN/GaN high electron mobility transistors *Appl. Phys. Lett.* **98** 023506

[14] Sawangsri K, Das P, Supardan S N, Mitrovic I Z, Hall S, Mahapatra R, Chakraborty A K, Treharne R, Gibbon J, Dhanak V R, Durose K and Chalker P R 2017 Experimental band alignment of Ta_2O_5/GaN for MIS-HEMT applications *Microelectron. Eng.* **178** 178–81

[15] Hansen P J, Vaithyanathan V, Wu Y, Mates T, Heikman S, Mishra U K, York R A, Schlom D G and Speck J S 2005 Rutile films grown by molecular beam epitaxy on GaN and AlGaN/GaN *J. Vac. Sci. Technol. B* **B23** 499–506

[16] Rawat A, Meer M, Surana V K, Bhardwaj N, Pendem V, Garigapati N S, Yadav Y, Ganguly S and Saha D 2018 Thermally grown TiO_2 and Al_2O_3 for GaN-Based MOS-HEMTs *IEEE Trans. Electron Devices* **65** 3725–31

[17] Nakano Y, Kachi T and Jimbo T 2003 Characteristics of SiO_2/n-GaN interfaces with β-Ga_2O_3 interlayers *Appl. Phys. Lett.* **83** 4336–8

[18] Yang S, Huang S, Schnee M, Zhao Q T, Schubert J and Chen K J 2013 Fabrication and characterization of enhancement-mode high-κ $LaLuO_3$-AlGaN/GaN MIS-HEMTs *IEEE Trans. Electron Devices* **60** 3040–6

[19] Cai Y, Zhou Y G, Chen K J and Lau K M 2005 III-nitride metal-insulator-semiconductor heterojunction field-effect transistors using sputtered AlON thin films *Appl. Phys. Lett.* **86** 032109

[20] Adivarahan V, Gaevski M, Sun W H, Fatima H, Koudymov A, Saygi S, Simin G, Yang J, Khan M A, Tarakji A, Shur M S and Gaska R 2003 Submicron gate Si_3N_4/AlGaN/GaN-metal-insulator-semiconductor heterostructure field-effect transistors *IEEE Electron Device Lett.* **24** 541–3

[21] Khan M A, Simin G, Yang J, Zhang J, Koudymov A, Shur M S, Gaska R, Hu X and Tarakji A 2003 Insulating gate III-N heterostructure field-effect transistors for high-power microwave and switching applications *IEEE Trans. Microw. Theory Tech.* **51** 624–33

[22] Hung T H, Esposto M and Rajan S 2011 Interfacial charge effects on electron transport in III-Nitride metal insulator semiconductor transistors *Appl. Phys. Lett.* **99** 162104

[23] Hung T H, Park P S, Krishnamoorthy S, Nath D N and Rajan

S 2014 Interface charge engineering for enhancement-mode GaN MISHEMTs *IEEE Electron Device Lett.* **35** 312–4

[24] Shin B, Weber J R, Long R D, Hurley P K, Van De Walle C G and McIntyre P C 2010 Origin and passivation of fixed charge in atomic layer deposited aluminum oxide gate insulators on chemically treated InGaAs substrates *Appl. Phys. Lett.* **96** 152908 -1-3

[25] Hashizume T, Ootomo S and Hasegawa H 2003 Suppression of current collapse in insulated gate AlGaN/GaN heterostructure field-effect transistors using ultrathin Al_2O_3 dielectric *Appl. Phys. Lett.* **83** 2952–4

[26] Robertson J and Falabretti B 2006 Band offsets of high k gate oxides on III-V semiconductors *J. Appl. Phys.* **100** 014111

[27] Hashizume T, Nishiguchi K, Kaneki S, Kuzmik J and Yatabe Z 2018 State of the art on gate insulation and surface passivation for GaN-based power HEMTs *Materials Science in Semiconductor Processing* **78** 85-95

[28] Hori Y, Mizue C and Hashizume T 2010 Process conditions for improvement of electrical properties of Al_2O_3/n-GaN structures prepared by atomic layer deposition *Jpn. J. Appl. Phys.* **49** 08001

[29] Chen J J, Gila B P, Hlad M, Gerger A, Ren F, Abernathy C R and Pearton S J 2006 Band offsets in the Sc_2O_3/GaN heterojunction system *Appl. Phys. Lett.* **88** 142115

[30] Liu C, Chor E F and Tan L S 2006 Structural and electrical characterizations of the pulsed-laser-deposition-grown Sc_2O_3/GaN heterostructure *Appl. Phys. Lett.* **88** 222113

[31] Liu C, Chor E F, Tan L S and Dong Y 2007 Band offset measurements of the pulsed-laser-deposition-grown Sc_2O_3 (111)/GaN (0001) heterostructure by X-ray photoelectron spectroscopy P*hys. Stat. Sol. (c)* **4** 2330–3

[32] Kraut E A, Grant R W, Waldrop J R and Kowalczyk S P 1983 Semiconductor core-level to valence-band maximum binding-energy differences: precise determination by x-ray photoelectron spectroscopy *Phys. Rev. B* **28** 1965–77

[33] Gila B P, Johnson J W, Mehandru R, Luo B, Onstine A H, Allums K K, Krishnamoorthy V, Bates S, C.R. Abernathy C R, Ren F, S.J. Pearton S J 2001 Gadolinium oxide and scandium oxide: gate dielectrics for GaN MOSFETs *Phys. Stat. Sol. (a)* **188** 239-242

[34] Afanas'ev VV, Shamuilia S, Badylevich M, Stesmans A, Edge LF, Tian W, Schlom D G, Lopes J M J, Roeckerath M and Schubert J 2007 Electronic structure of silicon interfaces with amorphous and epitaxial insulating oxides: Sc_2O_3, Lu_2O_3, $LaLuO_3$ *Microelectron Eng*. **84** 2278–81.

[35] Tippins H H 1966 Absorption edge spectrum of scandium oxide *J. Phys. Chem. Solids* **27** 1069-1071.

[36] Dixon S C, Jiamprasertboon A, Carmalt C J, Parkin I P 2018 Luminescence behaviour and deposition of Sc_2O_3 thin films from scandium (III) acetylacetonate at ambient pressure *Appl. Phys. Lett.* **112** 221902

[37] Moulder J F, Stickle W F, Sobol P E and Bomben K D 1992 *Handbook of X-ray photoelectron spectroscopy* ed Jill Chastain (USA: Perkin-Elmer Corporation, Physical Electronics Division) 0-9648124-1-X

[38] Woollam J A 2011 Woollam J A Co. Inc., New England, USA

[39] Das P, Jones L A H, Gibbon J T, Dhanak V R, Partida- T, Roberts J W, Potter R, Chalker P R, Cho S, Thayne G, Mahapatra R and Mitrovic I Z 2020 Band Line-up Investigation of Atomic Layer Deposited TiAlO and GaAlO on GaN *ECS J. Solid State Sci. Technol.* **9** 63003

[40] Shirley D A 1972 High-resolution X-ray photoemission spectrum of the valence bands of gold *Phys. Rev. B* **5** 4709

[41] Medenbach O, Dettmar D, Shannon R D, Fischer R X, Yen W M 2001 Refractive index and optical dispersion of rare earth oxides using a small-prism technique *J. Opt. A: Pure Appl. Opt.* **3** 174-177

[42] Shahrokhabadi H, Bananej A and Vaezzadeh M 2017 Investigation of Cody-Lorentz and Tauc-Lorentz models in characterizing dielectric function of $(HfO_2)_x(ZrO_2)_{1-x}$ mixed thin film *Journal of Applied Spectroscopy* **84** 915–922

[43] Wagner J, Obloh H, Kunzer M, Maier M, Köhler K and Johs B 2001 Dielectric function spectra of GaN, AlGaN, and GaN/AlGaN heterostructures *J. Appl. Phys.* **89** 2779

[44] Di M, Bersch E, Diebold A C, Consiglio S, Clark R D, Leusink G J and Kaack T 2011 Comparison of methods to determine bandgaps of ultrathin HfO_2 films using spectroscopic ellipsometry *J. Vac. Sci. Technol. A* **29**(4) 041001

[45] Fritsch D, Schmidt H and Grundmann M 2003 Band-structure pseudopotential calculation of zinc-blende and wurtzite AlN, GaN, and InN *Phys. Rev. B* **67** 235205

[46] Craft H S, Collazo R, Losego M D, Mita S, Sitar Z and Maria J P 2007 Band offsets and growth mode of molecular beam epitaxy grown MgO(111) on GaN(0002) by x-ray photoelectron spectroscopy *J. Appl. Phys.* **102** 074104

[47] Paisley E A, Brumbach M, Allerman A A, Atcitty S, Baca A G, Armstrong A M, Kaplar R J and Ihlefeld J F 2015 Spectroscopic investigations of band offsets of $MgO|Al_xGa_{1-x}N$ epitaxial heterostructures with varying AlN content *Appl. Phys. Lett.* **107** 102101

[48] Muth J F, Lee J H, Shmagin I K, Kolbas R M and Casey H C 1997 Absorption coefficient , energy gap , exciton binding energy and recombination lifetime of GaN obtained from transmission measurements *Appl. Phys. Lett.* **71** 2572

[49] Sun Q, Selloni A, Myers T H and Doolittle W A 2006 Oxygen adsorption and incorporation at irradiated GaN(0001) and GaN(0001) surfaces: first-principles density-functional calculations *Phys. Rev. B* **74** 195317

[50] Zywietz T K, Neugebauer J and Scheffler M 1999 The adsorption of oxygen at GaN surfaces *Appl. Phys. Lett.* **74** 1695–7

[51] Nichols M T, Li W, Pei D, Antonelli G A, Lin Q, Banna S, Nishi Y and Shohet J L 2014 Measurement of bandgap energies in low-k organosilicates *J. Appl. Phys.* **115** 094105

[52] Hosseini S, Vahedpour M, Shaterian M and Rezvani M A 2018 Investigation of structural and optoelectronic properties of Sc_2O_3 nanoclusters: a DFT study *Phys. Chem. Res*. **6** 493–504

[53] Almalki S, Tekin S B, Sedghi N, Hall S and Mitrovic I Z 2021 Applicability of Sc_2O_3 versus Al_2O_3 in MIM rectifiers for IR rectenna *Solid-State Electronics* **184** 108082 -1-4

[54] Zhang Z, Guo Y and Robertson J 2019 Microelectronic Engineering Atomic structure and band alignment at Al_2O_3/GaN, Sc_2O_3/GaN and La_2O_3/GaN interfaces : A first-principles study *Microelectron. Eng.* **216** 111039

[55] Ni J, Hu S, Li M, Jia F, Qin G, Li Q, Zhou Z, Zha F, Ren W and Wang Y 2022 Accurate band offset prediction of Sc_2O_3/GaN and θ-Al_2O_3/GaN heterojunctions using a dielectric-dependent hybrid functional *ACS Appl. Electron. Mater*. **4** 2747–52